# Vortex annihilation in the ordering kinetics of the O(2) model

Gene F. Mazenko and Robert A. Wickham
*The James Franck Institute and the Department of Physics, The University of Chicago, Chicago, Illinois 60637*
(Received 5 December 1996)

The vortex-vortex and vortex-antivortex correlation functions are determined for the two-dimensional O(2) model undergoing phase ordering. We find reasonably good agreement with experimental and simulation results for the vortex-vortex correlation function where there is a short-scaled distance depletion zone due to the repulsion of like-signed vortices. The vortex-antivortex correlation function agrees well with experimental and simulation results for intermediate- and long-scaled distances. At short-scaled distances the simulations and experiments show a depletion zone not seen in the theory. [S1063-651X(97)00205-5]

PACS number(s): 05.70.Ln, 64.60.Cn, 64.60.My, 64.75.+g

## I. INTRODUCTION

The late-stage ordering of systems in the process of breaking a continuous symmetry is dominated by the dynamics of topological defects. In the case of the $n$-vector model with the number of components $n$ of the order parameter equal to the spatial dimensionality $d$ one has point defects that are vortices for $n=2$ and monopoles for $n=3$ [1]. We focus mainly on the case $n=d=2$ here. Because of the conservation of topological charge, ordering in these systems occurs through the charge conserving process of vortex-antivortex annihilation. The statistical description of this annihilation process will be a central focus of this paper. We present here a calculation for the separate vortex-vortex and vortex-antivortex correlation functions. Knowledge of these functions is an important ingredient in understanding the vortex annihilation process. Since these functions contain detailed information about the vortex correlations, comparison of our results with simulation and experiment provides the most stringent test of the theory to date. In the original work [2] in this area only the signed defect correlation function was computed. The unsigned quantity is technically much more difficult to evaluate as we discuss in this paper. The comparison of the result for the signed quantity with experiments and simulations was confused by the use of a theory [3] that led to unphysical singularities at short distances in this quantity. The source of this singularity was recently uncovered by us [4] and the theory reorganized so as to give physical results for the signed defect correlation function. This development motivated us to make a renewed effort to evaluate the unsigned defect correlation function, with the results presented here.

We show in Fig. 1 the vortex-vortex correlation function for the two-dimensional O(2) model obtained from the theory developed here and from cell-dynamical simulations by Mondello and Goldenfeld [5]. Experiments by Nagaya *et al.* [6] on two-dimensionally aligned nematic liquid crystals, which mimic the O(2) model, have been able to measure the dynamical vortex correlations. The experimental data are also shown in Fig. 1. There is reasonable agreement between the theoretical curve and the data from experiment and simulation. All show a depletion zone at short-scaled distances for like-signed defects. This is expected on physical grounds since like-signed defects repel one another. It is nontrivial that we see evidence for a repulsive interaction. The vortex interactions emerge naturally in the theory from the equation of motion for the order parameter. In Fig. 2 we show the vortex-antivortex correlation function for theory, experiment [6], and simulation [5]. There is good agreement between the theory presented here and the experimental and simulation data at large- and intermediate-scaled distances. There is a clear discrepancy between theory and simulation results at short-scaled distances. The theory shows a monotonic behavior as the separation distance goes to zero. The simulation, however, shows a maximum at short separation distances and then falls rapidly to zero. Although somewhat noisy, the experimental data also have a depletion zone at short-scaled distances, in contrast to the theory. The depletion zone seen in the experimental and simulation data for the vortex-antivortex correlation function is harder to understand physically since the defect pair is attractive and headed toward annihilation. Some possible explanations will be presented in Sec. VIII. While the theory satisfies the sum rule implied by topological charge conservation, it does not appear that this general constraint is satisfied by the simulations.

## II. MODEL

We consider the $n$-vector model with O($n$) symmetry, which describes the dynamics of a nonconserved, $n$-component order-parameter field $\vec{\psi}(1)=(\psi_1(1),\ldots,\psi_n(1))$. Here we use the shorthand notation $1=(\mathbf{r}_1,t_1)$. The order parameter evolves *via* the time-dependent Ginzburg-Landau equation [3]

$$\frac{\partial\vec{\psi}}{\partial t}=\nabla^2\vec{\psi}-\frac{\partial V[\vec{\psi}]}{\partial\vec{\psi}}, \tag{2.1}$$

which can be derived from a free energy containing a square-gradient term and a potential term, $V[\vec{\psi}]$. We assume that the quench is to zero temperature where the usual noise term on the right-hand side of Eq. (2.1) is zero [7]. The potential $V[\vec{\psi}]$ is chosen to have O($n$) symmetry with a degenerate set of equilibrium minima at $\psi\equiv|\vec{\psi}|=\psi_0$. Since only these properties of $V[\vec{\psi}]$ will be important in what follows we need not be more specific in our choice for $V[\vec{\psi}]$. It is believed that our final results are independent of the exact na-

 

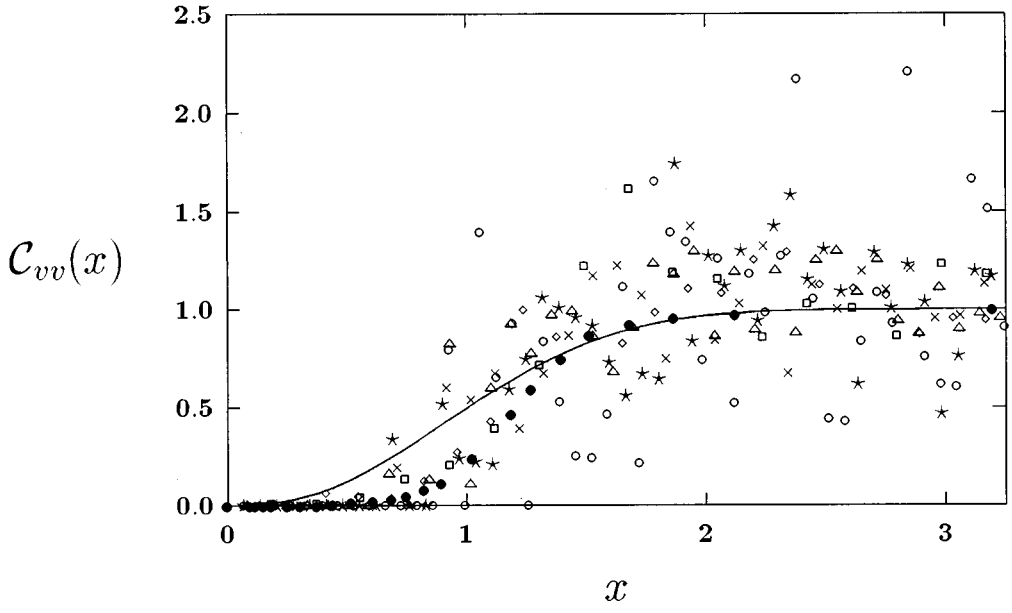


FIG. 1. The scaling form $\mathcal{C}_{vv}$ (3.19) as a function of the scaled length $x=r/L(t)$ for the vortex-vortex correlation function of the two-dimensional O(2) model. The solid curve is the result of the theory presented here. The solid dots (●) represent the simulation data of Mondello and Goldenfeld [5]. The experimental data of Nagaya *et al.* [6] on two-dimensionally aligned nematic liquid crystals are also shown. The experimental data were taken at times $t=4$ sec (□), $t=8$ sec (◇), $t=12$ sec (×), $t=16$ sec (△), $t=24$ sec (⋆), and $t=32$ sec (○) following the quench.

ture of the initial state, provided it is a disordered state. Indeed, it is well established [8] that for late times $t$ following a quench from the disordered to the ordered phase the dynamics obey scaling. In this regime, where order increases as the defects annihilate, the system can be described in terms of a single growing length $L(t)$, which is characteristic of the spacing between defects. At late times the order-parameter correlation function

$$C(12)\equiv\langle\vec{\psi}(1)\cdot\vec{\psi}(2)\rangle \tag{2.2}$$

has an equal-time scaling form

$$C(\mathbf{r},t)=\psi_0^2\mathcal{F}(x), \tag{2.3}$$

where $\mathcal{F}$ is a universal function, depending only on $n$ and $d$. The scaled length $x$ is defined as $x=r/L(t)$ with

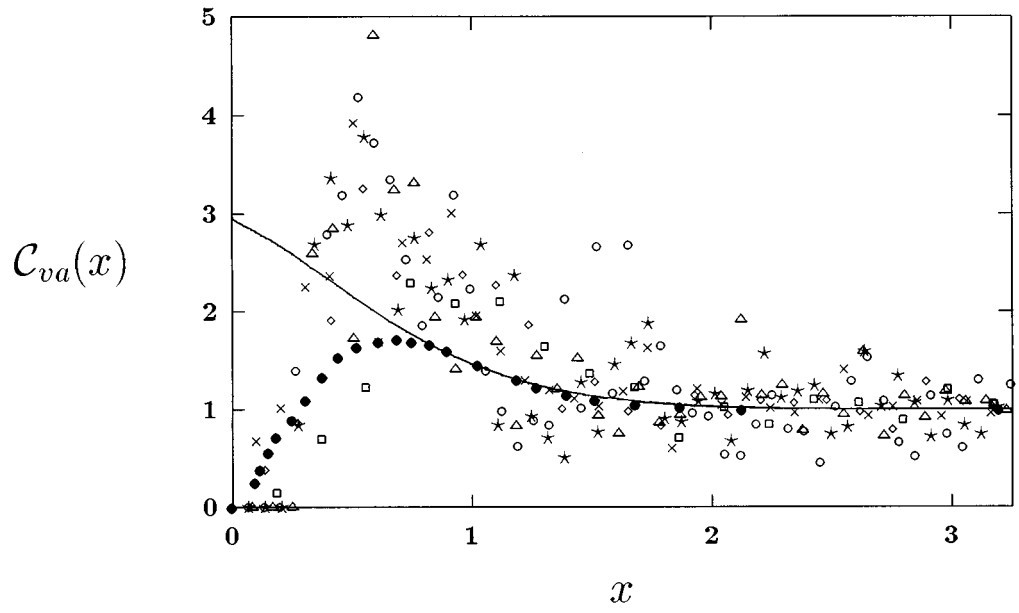


FIG. 2. The scaling form $\mathcal{C}_{va}$ (3.20) as a function of the scaled length $x=r/L(t)$ for the vortex-antivortex correlation function of the two-dimensional O(2) model. The solid curve and the symbols are defined as in Fig. 1. The abscissa of the simulation data [5] is scaled to give the best fit to the theory at intermediate to large $x$. The same rescaling factor for the simulation data is used in all the figures. No such rescaling of the experimental data [6] was necessary in any of the figures.

$r \equiv |\mathbf{r}| \equiv |\mathbf{r}_2 - \mathbf{r}_1|$. The scaling hypothesis states that all two-point correlation functions can be written as universal functions of $x$. It is also well established that, in the scaling regime, $L(t) \sim t^{\phi}$. For the nonconserved models considered here the exponent $\phi = 1/2$ [9].

### III. GENERAL FEATURES OF POINT DEFECTS

Let us briefly review the theoretical picture associated with topological point defects. The results of this section are quite general and hold independent of the particular dynamics, such as Eq. (2.1), or the approximation scheme, such as the Gaussian approximation, used to model the system. The vortex charge density can be written in the form

$$\rho(1) = \sum_{\alpha} q_{\alpha} \delta(\mathbf{r}_1 - \mathbf{x}_{\alpha}(t_1)), \tag{3.1}$$

where $\mathbf{x}_{\alpha}(t_1)$ is the position at time $t_1$ of the $\alpha$th point defect, which has a topological charge $q_{\alpha}$. We will restrict the analysis here to the case of charge $\pm 1$ vortices where $q_{\alpha}^2 = 1$. This case dominates the late-stage ordering since higher-charged defects are energetically unfavorable and dissociate into charge $\pm 1$ defects early on.

The next step is to note, as pointed out by Halperin [10], that the positions of defects are located by the zeros of the order-parameter field $\vec{\psi}$. Therefore the charged or signed density for point defects is given by

$$\rho(1) = \delta(\vec{\psi}(1)) \mathcal{D}(1), \tag{3.2}$$

where the Jacobian $\mathcal{D}$ associated with the change of variables from the set of vortex positions to the field $\vec{\psi}$ is defined by

$$\mathcal{D}(1) = \frac{1}{n!} \epsilon_{\mu_1, \mu_2, \ldots, \mu_n} \epsilon_{\nu_1, \nu_2, \ldots, \nu_n} \times \nabla_{\mu_1} \psi_{\nu_1} \nabla_{\mu_2} \psi_{\nu_2} \cdots \nabla_{\mu_n} \psi_{\nu_n}, \tag{3.3}$$

where $\epsilon_{\mu_1, \mu_2, \ldots, \mu_n}$ is the $n$-dimensional fully antisymmetric tensor and summation over repeated indices is implied. The unsigned density, $n(1)$, does not consider the charge of the defect and is given by

$$n(1) = \sum_{\alpha} \delta(\mathbf{r}_1 - \mathbf{x}_{\alpha}(t_1)) = \delta[\vec{\psi}(1)] |\mathcal{D}(1)|. \tag{3.4}$$

If we have products of such densities at equal times, $t_1 = t_2 = t$, we write

$$\rho(1)\rho(2) = \delta(\mathbf{r}_1 - \mathbf{r}_2) \sum_{\alpha} \delta(\mathbf{r}_1 - \mathbf{x}_{\alpha}(t)) + \tilde{\rho}(1)\tilde{\rho}(2). \tag{3.5}$$

We use the tildes in Eq. (3.5) to indicate that the product $\tilde{\rho}(1)\tilde{\rho}(2)$ contains only terms arising from different defects. We can also write

$$\rho(1)\rho(2) = \delta(\mathbf{r}_1 - \mathbf{r}_2) n(1) + \tilde{\rho}(1)\tilde{\rho}(2). \tag{3.6}$$

The equal-time charged or signed defect correlation function is given by the average of Eq. (3.6)

$$G_s(\mathbf{r}, t) = \langle \rho(1)\rho(2) \rangle = n_0(t)\, \delta(\mathbf{r}) + \tilde{G}_s(\mathbf{r}, t). \tag{3.7}$$

The first term in Eq. (3.7) represents self-correlations and

$$n_0(t) = \langle n(1) \rangle \tag{3.8}$$

is the average unsigned point defect density at time $t$ [11]. The second term in Eq. (3.7) is

$$\tilde{G}_s(\mathbf{r}, t) = \langle \tilde{\rho}(1)\tilde{\rho}(2) \rangle \tag{3.9}$$

and measures the signed correlation between different defects. It is easy to see that the signed defect correlation function, $G_s$, can also be decomposed as

$$G_s = 2C_{vv} - 2C_{va}, \tag{3.10}$$

where $C_{vv}$ is the correlation function between like-signed vortices and $C_{va}$ is the correlation function between vortices and antivortices.

We define the equal-time unsigned defect correlation function as

$$G_u(\mathbf{r}, t) = \langle n(1)n(2) \rangle = n_0(t)\, \delta(\mathbf{r}) + \tilde{G}_u(\mathbf{r}, t) \tag{3.11}$$

with

$$\tilde{G}_u(\mathbf{r}, t) = \langle \tilde{n}(1)\tilde{n}(2) \rangle. \tag{3.12}$$

As with the signed quantity, one can write $G_u$ in terms of the vortex-vortex and vortex-antivortex correlation functions:

$$G_u = 2C_{vv} + 2C_{va}. \tag{3.13}$$

Inverting Eqs. (3.10) and (3.13) and using Eqs. (3.7) and (3.11) one has

$$C_{vv}(\mathbf{r}, t) = \tfrac{1}{2}\, n_0(t)\, \delta(\mathbf{r}) + \tilde{C}_{vv}(\mathbf{r}, t), \tag{3.14}$$

$$C_{va}(\mathbf{r}, t) = \tfrac{1}{4} [\tilde{G}_u(\mathbf{r}, t) - \tilde{G}_s(\mathbf{r}, t)], \tag{3.15}$$

where

$$\tilde{C}_{vv}(\mathbf{r}, t) = \tfrac{1}{4} [\tilde{G}_s(\mathbf{r}, t) + \tilde{G}_u(\mathbf{r}, t)]. \tag{3.16}$$

As one would expect, for the vortex-antivortex correlations, there is no $\delta$-function contribution from self-correlations.

We are interested in the correlations between different vortices and antivortices in the scaling regime, where the correlations assume scaling form dependent only on the scaled length $x$. We define

$$\mathcal{G}_s(x) \equiv \frac{\tilde{G}_s(\mathbf{r}, t)}{[n_0(t)]^2}, \tag{3.17}$$

$$\mathcal{G}_u(x) \equiv \frac{\tilde{G}_u(\mathbf{r}, t)}{[n_0(t)]^2}, \tag{3.18}$$

$$\mathcal{C}_{vv}(x) \equiv \frac{4\tilde{C}_{vv}(\mathbf{r}, t)}{[n_0(t)]^2} = \mathcal{G}_s(x) + \mathcal{G}_u(x), \tag{3.19}$$

$$\mathcal{C}_{va}(x) \equiv \frac{4C_{va}(\mathbf{r}, t)}{[n_0(t)]^2} = \mathcal{G}_u(x) - \mathcal{G}_s(x). \tag{3.20}$$

Both $\mathcal{C}_{vv}(x)$ and $\mathcal{C}_{va}(x)$ are normalized to approach 1 as $x\to\infty$.

Since the topological charge is conserved, one has the very important constraint [10,11]

$$\int d^d r G_s(\mathbf{r},t)=0. \tag{3.21}$$

Using Eq. (3.7) this conservation law can be written in the form

$$\int d^d r \widetilde{G}_s(\mathbf{r},t)=-n_0(t). \tag{3.22}$$

Theory, simulation, and experiment indicate that the scaling results (3.17)–(3.20) and the result

$$n_0(t)=\frac{A}{L^d(t)}, \tag{3.23}$$

where $A$ is a constant, hold. Inserting these results in Eq. (3.22) leads to the relation

$$\int d^d x \mathcal{G}_s(x)=-\frac{1}{A}. \tag{3.24}$$

A measurement of $n_0(t)$ and a choice for $L(t)$ fixes $A$, allowing one to check that the sum rule (3.24) is satisfied. As shown in [2] our theoretical results satisfy this sum rule exactly.

The results presented above are rather general. To evaluate $G_s$ explicitly one can use the Gaussian closure approximation, as was done in [2]. The evaluation of $G_u$ in this same approximation is technically much more difficult than the calculation of $G_s$ because of the absolute value sign in the definition (3.4) of the unsigned defect density $n(1)$. The purpose of this paper is to compute $G_u$ and thereby obtain $C_{vv}$ and $C_{va}$. In Secs. VI and VII we carry out this calculation with explicit results for $n=d=2$. First, however, we must briefly review the calculations of the order-parameter scaling function and the signed defect correlation function within the Gaussian closure approximation.

## IV. THE GAUSSIAN CLOSURE APPROXIMATION

Substantial progress has been made in determining the order-parameter scaling function $\mathcal{F}$ using the theory developed in [12]. In this and related theories, one expresses the order parameter $\vec{\psi}(\mathbf{r},t)$ as a local nonlinear function of an auxiliary field $\vec{m}(\mathbf{r},t)$, which is physically interpreted as the distance, at time $t$, from position $\mathbf{r}$ to the closest defect. One of the physical motivations for introducing $\vec{m}(\mathbf{r},t)$ is that it is *smoother* than the order-parameter field. Sharp interfaces or well-defined defects produce a nonanalytic structure in the order-parameter scaling function $\mathcal{F}(x)$ at small-scaled distances $x$, which is responsible for the Porod's law decay seen in scattering experiments [13]. The expectation, however, is that the auxiliary field correlation function $f(x)$, defined below, will be analytic in this same distance range. In the case of a scalar order parameter these expectations are supported by the theory [12]. However, for the simplest theory [3] with $n>1$ this is not the case. One finds a weak nonanalytic component in $f$ and, more significantly, for $n=2$ one can trace this non-analytic component to an unphysical divergence [2] in the scaling form for the signed vortex correlation function $\mathcal{G}_s(x)$ at small $x$. In previous work [4] for $n=2$ we showed how these problems can be resolved by taking seriously the assumption that the correlations of the auxiliary field are indeed smoother than those of the order parameter. We find that it is possible to rearrange the theory such that $f$ is analytic in $x$ if we extend the theory to include fluctuations about the ordering field and treat the separation between the ordering field and the fluctuation field carefully.

More specifically we can decompose the order parameter $\vec{\psi}$ as

$$\vec{\psi}=\vec{\sigma}[\vec{m}]+\vec{u}. \tag{4.1}$$

$\vec{\sigma}$ is chosen to reflect the defect structure in the problem and is of $O(1)$. $\vec{u}$ represents fluctuations about the ordering field $\vec{\sigma}$ and is of $O(L^{-2})$ at late times. The defect structure is incorporated by demanding that $\vec{\sigma}$ satisfy the Euler-Lagrange equation for the order parameter around a static defect in equilibrium. This determines $\vec{\sigma}$ as a function of $\vec{m}$. Since we expect only the lowest-energy defects, having unit topological charge, will survive to late times we obtain [3]

$$\vec{\sigma}[\vec{m}]=A(m)\hat{m}. \tag{4.2}$$

In [3] it was shown that $A$ increases linearly from zero near the defect core and relaxes algebraically to its ordered value $A=\psi_0$ for large $m\equiv|\vec{m}|$.

Evolution under Eq. (2.1) causes $\vec{\psi}$ to order and assume a distribution that is far from Gaussian. However, it is reasonable to assume that the probability distribution for the auxiliary field $\vec{m}$ will be near a Gaussian. Indeed, a simple and successful assumption [14] to make is that the probability distribution for $\vec{m}$ is Gaussian with the correlation function $C_0(12)$ explicitly defined through

$$\langle m_i(1)m_j(2)\rangle=\delta_{ij}C_0(12). \tag{4.3}$$

The system is assumed to be statistically isotropic and homogeneous so $C_0(12)$ is invariant under interchange of its spatial indices. For future reference we also define the one-point correlation function

$$S_0(1)=C_0(11) \tag{4.4}$$

and the normalized correlation function

$$f(12)=\frac{C_0(12)}{\sqrt{S_0(1)S_0(2)}}. \tag{4.5}$$

Since $m$ measures the characteristic distance between defects it is expected to grow as $L$ in the late-time scaling regime. This means that $C_0$ and $S_0$ grow as $L^2$ at late times.

If $\vec{m}$ is treated as a Gaussian variable then its probability distribution is characterized by the single function $f$. This function can be determined by requiring that the equation of motion for $\vec{\sigma}$ be satisfied on average. In [4] it was shown that

for $n=2$ this requirement produces the following late-time scaling equation for the equal-time order-parameter correlations:

$$\vec{x}\cdot\vec{\nabla}_x\mathcal{F}+\nabla_x^2\mathcal{F}-\frac{\pi}{4\mu}\mathcal{F}+\frac{\pi}{2\mu}f\partial_f\mathcal{F}=0, \tag{4.6}$$

where, for general $n$, $\mathcal{F}$ is related to $f$ *via*

$$\mathcal{F}=\frac{nf}{2\pi}B^2\left(\frac{1}{2},\frac{n+1}{2}\right)F\left(\frac{1}{2},\frac{1}{2};\frac{n+2}{2};f^2\right). \tag{4.7}$$

Here $B$ is the beta function and $F$ is the hypergeometric function [3,15]. In the derivation of Eq. (4.6) we have defined the scaling length

$$L^2(t)=\frac{\pi S_0(t)}{2\mu}=4t. \tag{4.8}$$

With the theory in this form there will be no leading small-$x$ nonanalyticities in the normalized auxiliary field correlation function $f$ and the small-$x$ divergence in the scaling form for the signed vortex correlation function found in earlier theories does not appear. The calculation of the scaling form for $\mathcal{F}$ (and thus $f$) reduces to the solution of the nonlinear eigenvalue problem (4.6) with the eigenvalue $\mu$. The eigenvalue is selected by numerically [4] finding the solution of Eq. (4.6), which satisfies the analytically determined boundary behavior at both large and small $x$.

## V. THE SIGNED DEFECT CORRELATION FUNCTION

The calculation of $G_s(\mathbf{r},t)$ (3.7), carried out in [2], begins with the observation that $\vec{\psi}$ and $\vec{m}$ share the same zeros, and that near these zeros we can use Eq. (4.2) to write

$$\vec{\psi}=a_0\vec{m}+b_0m^2\vec{m}+\cdots, \tag{5.1}$$

where $a_0$ and $b_0$ are constants that depend on the potential. It is then easy to see that in Eqs. (3.2) and (3.4) for $\rho(1)$ and $n(1)$ we can replace $\vec{\psi}(1)$ with $\vec{m}(1)$ and the factors of $a_0$ and $b_0$ all cancel. Then, assuming $\vec{m}$ is a Gaussian field, it is straightforward to see that $\widetilde{G}_s(\mathbf{r},t)$ (3.9) factors into a product of Gaussian averages, which can be evaluated using standard methods. One then finds that $\widetilde{G}_s(\mathbf{r},t)$ indeed has the scaling form (3.17) with $\mathcal{G}_s(x)$ given by [16]

$$\mathcal{G}_s(x)=\frac{\Gamma^2(1+n/2)}{n!}\left(\frac{8\mu}{S^{(2)}}\right)^n\left[\frac{h(x)}{x}\right]^{n-1}\frac{\partial h(x)}{\partial x} \tag{5.2}$$

with

$$h=-\frac{\gamma f'}{2\pi}, \tag{5.3}$$

$$\gamma=\frac{1}{\sqrt{1-f^2}}, \tag{5.4}$$

and

$$S^{(2)}\equiv\frac{1}{n^2}\langle[\vec{\nabla}\vec{m}]^2\rangle=\frac{1}{n} \tag{5.5}$$

in this theory. The defect density is given by

$$n_0(t)=\frac{n!}{2^{n/2}\Gamma(1+n/2)}\left[\frac{S^{(2)}}{2\pi S_0(t)}\right]^{n/2}. \tag{5.6}$$

Equation (5.6) leads to the result $n_0\sim L^{-n}$, which is just a restatement that there is scaling in the problem governed by the single length $L(t)$.

Since $f$ is determined in the theory for the order-parameter correlation function, the function $G_s(\mathbf{r},t)$ is fully determined in the scaling regime. The derivatives in Eqs. (5.2) and (5.3) make $\mathcal{G}_s(x)$ a rather sensitive function of $f(x)$ for small $x$.

## VI. CALCULATION OF $\widetilde{G}_u$

The equal-time unsigned defect correlation function $G_u(\mathbf{r},t)$ (3.11) can be evaluated through a series of steps. We work with general $n$. The average that needs to be computed is Eq. (3.12):

$$\widetilde{G}_u(\mathbf{r},t)=\langle\delta[\vec{\psi}(1)]|\mathcal{D}(1)|\delta[\vec{\psi}(2)]|\mathcal{D}(2)|\rangle. \tag{6.1}$$

The first step is to realize that one can replace $\vec{\psi}$ by $\vec{m}$ in Eq. (6.1) and write $\widetilde{G}_u$ in terms of integrals over the reduced probability distribution $G(\xi_1,\xi_2)$:

$$\widetilde{G}_u(\mathbf{r},t)=\int\prod_{\mu\nu}d(\xi_1)_\mu^\nu d(\xi_2)_\mu^\nu|\mathcal{D}(\xi_1)||\mathcal{D}(\xi_2)|G(\xi_1,\xi_2), \tag{6.2}$$

where

$$\mathcal{D}(\xi)=\frac{1}{n!}\epsilon_{\mu_1,\mu_2,\ldots,\mu_n}\epsilon_{\nu_1,\nu_2,\ldots,\nu_n}\xi_{\mu_1}^{\nu_1}\xi_{\mu_2}^{\nu_2}\cdots\xi_{\mu_n}^{\nu_n} \tag{6.3}$$

and

$$G(\xi_1,\xi_2)=\left\langle\delta[\vec{m}(1)]\delta[\vec{m}(2)]\prod_{\mu\nu}\delta[(\xi_1)_\mu^\nu-\nabla_\mu m_\nu(1)]\times\delta[(\xi_2)_\mu^\nu-\nabla_\mu m_\nu(2)]\right\rangle. \tag{6.4}$$

The indices $\mu$ and $\nu$ range from 1 to $n$, unless stated otherwise. The Gaussian average defining $G(\xi_1,\xi_2)$ is calculated in Appendix A. It is shown there how one can write $G(\xi_1,\xi_2)$ in terms of the longitudinal and transverse components of the rotated variables $(t_j)_\mu^\nu$ $(j=1\text{or }2)$ defined by

$$(t_j)_\mu^\nu=\hat{M}_\beta^\mu(\xi_j)_\beta^\nu, \tag{6.5}$$

where $\hat{M}$ is an orthogonal matrix. We define the longitudinal piece of $t_j$ as $(t_j)_L^\nu\equiv(t_j)_1^\nu$ and write $(t_j)_T$ to denote the transverse pieces: $(t_j)_\mu^\nu$ with $\mu>1$. One then obtains

$$G(t_1,t_2)=\left(\frac{\gamma}{2\pi S_0}\right)^n G_L((\vec{t}_1)_L,(\vec{t}_2)_L)G_T((t_1)_T,(t_2)_T), \tag{6.6}$$

where

$$G_L((\vec{t}_1)_L,(\vec{t}_2)_L)=\left(\frac{\gamma_L}{2\pi S_L}\right)^n \exp-\frac{\gamma_L^2}{2S_L} \times\left[\sum_j (\vec{t}_j)_L^2-2f_L(\vec{t}_1)_L\cdot(\vec{t}_2)_L\right], \tag{6.7}$$

$$G_T((t_1)_T,(t_2)_T)=\left(\frac{\gamma_T}{2\pi S_T}\right)^{n(n-1)} \exp-\frac{\gamma_T^2}{2S_T} \times\left[\sum_{\mu=2}\sum_{\nu j}[(t_j)_\mu^\nu]^2 -2f_T\sum_{\mu=2}\sum_\nu (t_1)_\mu^\nu(t_2)_\mu^\nu\right]. \tag{6.8}$$

The longitudinal quantities $S_L$, $f_L$, and $\gamma_L$ are defined in terms of $C_0$ and $S_0$ through

$$S_L=S^{(2)}-\frac{\gamma^2}{S_0}(C_0')^2, \tag{6.9}$$

$$C_L=-C_0''-\frac{f\gamma^2}{S_0}(C_0')^2, \tag{6.10}$$

$$f_L=\frac{C_L}{S_L}, \tag{6.11}$$

$$\gamma_L^2=(1-f_L^2)^{-1}. \tag{6.12}$$

The corresponding transverse functions are

$$S_T=S^{(2)}, \tag{6.13}$$

$$C_T=-\frac{C_0'}{r}, \tag{6.14}$$

$$f_T=\frac{C_T}{S_T}, \tag{6.15}$$

$$\gamma_T^2=(1-f_T^2)^{-1}. \tag{6.16}$$

Since the matrix $\hat{M}$ is orthogonal we have

$$\mathcal{D}(\xi_j)=\mathcal{D}(t_j) \tag{6.17}$$

so we may write

$$\widetilde{G}_u(\mathbf{r},t)=\int\prod_{\mu\nu} d(t_1)_\mu^\nu d(t_2)_\mu^\nu|\mathcal{D}(t_1)||\mathcal{D}(t_2)|\left(\frac{\gamma}{2\pi S_0}\right)^n \times G_L((\vec{t}_1)_L,(\vec{t}_2)_L)G_T((t_1)_T,(t_2)_T). \tag{6.18}$$

Under the change of variables,

$$(\vec{t}_j)_L=\sqrt{\frac{S_L}{\gamma_L^2}}(\vec{s}_j)_L \tag{6.19}$$

and, for $\mu>1$,

$$(t_j)_\mu^\nu=\sqrt{\frac{S_T}{\gamma_T^2}}(s_j)_\mu^\nu, \tag{6.20}$$

$\widetilde{G}_u(\mathbf{r},t)$ becomes

$$\widetilde{G}_u(\mathbf{r},t)=\left(\frac{\gamma}{2\pi S_0}\right)^n \frac{S_L(S_T)^{n-1}}{(2\pi)^{n^2}}\gamma_L^{-(n+2)}\gamma_T^{-(n+2)(n-1)} \times\mathcal{N}(f_T,f_L), \tag{6.21}$$

where

$$\mathcal{N}(f_T,f_L)=\int\prod_{\mu\nu} d(s_1)_\mu^\nu d(s_2)_\mu^\nu|\mathcal{D}(s_1)||\mathcal{D}(s_2)| \times\exp-\frac{1}{2}[(\vec{s}_1)_L^2+(\vec{s}_2)_L^2-2f_L(\vec{s}_1)_L\cdot(\vec{s}_2)_L] \times\exp-\frac{1}{2}\sum_{\mu=2}\sum_\nu\{[(s_1)_\mu^\nu]^2+[(s_2)_\mu^\nu]^2 -2f_T(s_1)_\mu^\nu(s_2)_\mu^\nu\}. \tag{6.22}$$

Equation (6.21), with the definition (6.22), is one of the central results of this paper. If we had taken this route in evaluating $\widetilde{G}_s$ we would have arrived at these same equations, only without the absolute value signs in Eq. (6.22). In the next section we will examine the $n=d=2$ case and go further to derive an expression for $\widetilde{G}_u$ that is convenient for numerical work.

However, first we examine the general expression (6.21) for $\widetilde{G}_u$ in the small-$x$ limit. We show in Appendix B that, in the scaling regime, as $x\to 0$, $f_T\to 1$ and, surprisingly, $f_L\to -1$. To examine this limit for $\widetilde{G}_u$ we make the change of variables

$$(s_1)_\mu^\nu=\frac{1}{\sqrt{\epsilon_T}}\phi_\mu^\nu+\frac{1}{2}\chi_\mu^\nu, \tag{6.23}$$

$$(s_2)_\mu^\nu=\frac{1}{\sqrt{\epsilon_T}}\phi_\mu^\nu-\frac{1}{2}\chi_\mu^\nu \tag{6.24}$$

for $\mu>1$ with

$$\epsilon_T=2(1-f_T) \tag{6.25}$$

and, for $\mu=1$,

$$(s_1)_L^\nu=-\frac{1}{\sqrt{\epsilon_L}}\phi_L^\nu+\frac{1}{2}\chi_L^\nu, \tag{6.26}$$

$$(s_2)_L^\nu=\frac{1}{\sqrt{\epsilon_L}}\phi_L^\nu+\frac{1}{2}\chi_L^\nu, \tag{6.27}$$

with

$$\epsilon_L = 2(1+f_L). \tag{6.28}$$

Then as $\epsilon_T$ and $\epsilon_L$ go to zero the arguments of the exponentials in Eq. (6.22) go over to

$$[(s_1)_\mu^\nu]^2+[(s_2)_\mu^\nu]^2-2f_T(s_1)_\mu^\nu(s_2)_\mu^\nu=[\phi_\mu^\nu]^2+[\chi_\mu^\nu]^2 \tag{6.29}$$

for $\mu>1$ and

$$(\vec{s}_1)_L^2+(\vec{s}_2)_L^2-2f_L(\vec{s}_1)_L\cdot(\vec{s}_2)_L=[\vec{\phi}_L]^2+[\vec{\chi}_L]^2 \tag{6.30}$$

for $\mu=1$. The important point is that, as $\epsilon_L$ and $\epsilon_T$ go to zero, the Jacobians $\mathcal{D}$ transform as

$$\mathcal{D}(s_1)=\frac{-1}{\sqrt{\epsilon_L}}\frac{1}{(\epsilon_T)^{(n-1)/2}}\mathcal{D}(\phi), \tag{6.31}$$

$$\mathcal{D}(s_2)=\frac{1}{\sqrt{\epsilon_L}}\frac{1}{(\epsilon_T)^{(n-1)/2}}\mathcal{D}(\phi). \tag{6.32}$$

Thus the Jacobians differ only by a sign in this limit and we have

$$|\mathcal{D}(s_1)||\mathcal{D}(s_2)|=-\mathcal{D}(s_1)\mathcal{D}(s_2) \tag{6.33}$$

as $x\to 0$. Since the scaling form for the unsigned defect correlation function $\mathcal{G}_s(x)$ is, up to a factor of $[n_0(t)]^2$, given by Eqs. (6.21) and (6.22) without the absolute value signs we see that $\mathcal{G}_u(x)$ differs from $\mathcal{G}_s(x)$ only by a sign

$$\mathcal{G}_u=-\mathcal{G}_s \tag{6.34}$$

as $x\to 0$. The relations (3.19) and (3.20) then lead to the results

$$\lim_{x\to 0}\mathcal{C}_{vv}(x)=0 \tag{6.35}$$

and

$$\lim_{x\to 0}\mathcal{C}_{va}(x)=-2\mathcal{G}_s(0). \tag{6.36}$$

Thus there is a depletion zone at short-scaled distances for like-signed defects. From previous work we know that $\mathcal{G}_s(0)<0$ [4] so the theory gives a nonzero, positive correlation at short-scaled distances for unlike-signed defects. These are general results and depend only on the Gaussian assumption, used to derive Eq. (6.21), and the particular small-$x$ behavior of $f$, which, as is shown in Appendix C, determines the small-$x$ behavior of the quantities $f_T$ and $f_L$.

## VII. TWO-DIMENSIONAL O(2) MODEL

We have not yet been able to explicitly evaluate $\mathcal{G}_u(x)$ for general $n=d$, except for small and large $x$. Here we specialize to $n=d=2$. Much theoretical work has recently been done on this case and detailed results are available for the auxiliary field correlation function $f(x)$. An additional motivation for examining this case is that simulation and experimental results exist for the vortex-vortex and vortex-antivortex correlation functions.

If we now specialize Eqs. (6.21) and (6.22) to $n=d=2$ then the unsigned vortex correlation function is given by

$$\tilde{G}_u(\mathbf{r},t)=[n_0(t)]^2\frac{2\gamma^2 S_L}{(2\pi)^4}\gamma_L^{-4}\gamma_T^{-4}\mathcal{N}(f_T,f_L) \tag{7.1}$$

with

$$\mathcal{N}(f_T,f_L)=\int d^2s_1d^2s_2J(\vec{s}_1,\vec{s}_2) \times\exp(-\tfrac{1}{2}[\vec{s}_1{}^2+\vec{s}_2{}^2-2f_L\vec{s}_1\cdot\vec{s}_2]), \tag{7.2}$$

where

$$J(\vec{s}_1,\vec{s}_2)=\int d^2xd^2y|s_{11}x_2-s_{12}x_1||s_{21}y_2-s_{22}y_1| \times\exp(-\tfrac{1}{2}[\vec{x}^2+\vec{y}^2-2f_T\vec{x}\cdot\vec{y}]). \tag{7.3}$$

We have simplified the notation by writing $\vec{s}_i$ in place of $(\vec{s}_i)_L$ and using $\vec{x}$ and $\vec{y}$ in place of $(\vec{s}_1)_T$ and $(\vec{s}_2)_T$, respectively. The $j$th component of $\vec{s}_i$ is written $s_{ij}$. The quantity $J$ is evaluated in Appendix B with the clean result

$$J(\vec{s}_1,\vec{s}_2)=2\pi\gamma_T^4|\vec{s}_1||\vec{s}_2|\tilde{J}(g), \tag{7.4}$$

where

$$\tilde{J}(g)=4\sqrt{1-g}+4\sqrt{g}\tan^{-1}\sqrt{\frac{g}{1-g}} \tag{7.5}$$

and

$$g=f_T^2(\hat{s}_1\cdot\hat{s}_2)^2. \tag{7.6}$$

Notice that $g$ depends only on the angle between $\vec{s}_1$ and $\vec{s}_2$ and not on their magnitudes. We can then separate Eq. (7.2) into an integration over magnitudes, followed by an overall integration over the angular piece:

$$\mathcal{N}(f_T,f_L)=(2\pi)^2\gamma_T^4\int_0^{2\pi}d\theta\tilde{J}(g)\int_0^\infty ds_1ds_2s_1^2s_2^2 \times\exp(-\tfrac{1}{2}[s_1^2+s_2^2-2g_Ls_1s_2]), \tag{7.7}$$

where we have defined

$$g_L=f_L\hat{s}_1\cdot\hat{s}_2 \tag{7.8}$$

and $\hat{s}_1\cdot\hat{s}_2=\cos\theta$. Expanding the exponential in Eq. (7.7) as a power series in $g_L$ and performing the integrations over the magnitudes $s_1$ and $s_2$ we obtain

$$\mathcal{N}(f_T,f_L)=(2\pi)^2\gamma_T^4\int_0^{2\pi}d\theta\tilde{J}(g) \times\sum_{l=0}^\infty\frac{(g_L)^l}{l!}2^{l+1}\Gamma^2\left(\frac{l+3}{2}\right). \tag{7.9}$$

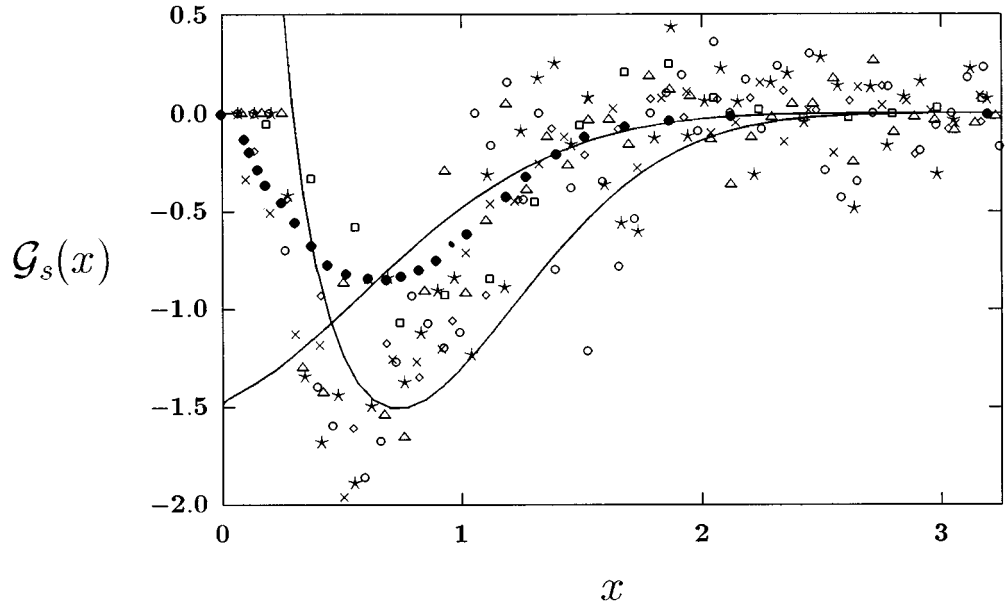


FIG. 3. The scaling form $\mathcal{G}_s$ (3.17) as a function of the scaled length $x=r/L(t)$ for the signed vortex correlation function of the two-dimensional O(2) model. At $x=1$ the lower solid curve is the prediction of the original theory [2,3] that does not treat fluctuations, and the upper solid curve is the result for the theory presented here, which does include fluctuations. The symbols are defined as in Fig. 1.

The symmetries of $g$ and $g_L$ under $\theta\to\theta-\pi$ allow us to restrict the region of integration in Eq. (7.9) and we use the definition (3.18) for the scaling form to write the final result for $\mathcal{G}_u$:

$$\mathcal{G}_u(x)=\frac{2\gamma^2 S_L\gamma_L^{-4}}{\pi^2}\int_0^{\pi/2}d\theta\widetilde{J}(g)\times\sum_{l=0}^{\infty}\frac{(g_L)^{2l}}{(2l)!}2^{2l+1}\Gamma^2\left(\frac{2l+3}{2}\right),\qquad(7.10)$$

where $S_L$, $f_L$, and $f_T$ are now functions of the scaled length $x$. The integral over $\theta$ and the sum over $l$ have to be evaluated numerically.

For large $x$ the functions $f$, $f_T$, and $f_L$ are all small and Eq. (7.10) simplifies since only the first two terms in the series need to be retained to give the essential physical features. In this limit the integral over $\theta$ is easily performed and one has

$$\mathcal{G}_u=1+f^2+\frac{1}{4}(f_L^2+f_T^2)-\frac{4\mu}{\pi}(f')^2.\qquad(7.11)$$

Since all of $f$, $f_T$, and $f_L$ decay as $e^{-x^2/2}$ for large $x$ [4], $\mathcal{G}_u$ rapidly approaches 1 as $x$ increases.

## VIII. COMPARISON OF THEORY AND SIMULATION

In our previous work [4] we numerically solved the eigenvalue problem (4.6) and determined the function $f(x)$ representing the scaling form for correlations in the auxiliary field. With this information we can use Eq. (7.10) to determine $\mathcal{G}_u(x)$ since for each $x$ at which we know $f(x)$ we can calculate $f_L$, $f_T$, and $S_L$ and perform the sum over $l$ and then the integration over $\theta$. The sum diverges as $|g_L|\to 1$ ($x\to 0$ and $\theta\to 0$) but since the smallest $x$ we consider is $x=0.0001$ this is not a real problem—we just have to sum up more terms to achieve a set accuracy. The integration over $\theta$ is straightforwardly accomplished using an open Newton-Cotes algorithm.

Using the relations (3.19) and (3.20) we have calculated the results for $\mathcal{C}_{vv}(x)$ and $\mathcal{C}_{va}(x)$, which are presented in Figs. 1 and 2, respectively. As expected, $\mathcal{C}_{vv}(x)$ has a depletion zone at small $x$, which has a characteristic size $x\approx 1$ [$|\mathbf{r}|\approx L(t)$]. In contrast, $\mathcal{C}_{va}(x)$ shows enhanced correlations in the same range of $x$. We present the results for $\mathcal{G}_s$ and $\mathcal{G}_u$ in Figs. 3 and 4. Also shown in Fig. 3 is the result of the earlier theory [2,3] for $\mathcal{G}_s$, which displays the divergence resulting from neglecting fluctuations. These four figures display the main results of this paper.

Also shown in these figures are the results of Mondello and Goldenfeld's cell-dynamics simulation [5], based on the time-dependent Ginzburg-Landau equation for the O(2) model. The lattice size used was $512\times 512$. The simulation data for the scaling forms of the vortex-vortex and vortex-antivortex correlation functions were taken directly from Figs. 8 and 9 of [5]. The experimental data of Nagaya *et al.* [6] are also shown. Relations (3.19) and (3.20) were used to calculate $\mathcal{G}_s$ and $\mathcal{G}_u$ for simulation and experiment. There is only one adjustable parameter in all these fits, which is the (unknown) proportionality coefficient between the scaling length $L(t)$ used in the theory and that used in experiments and simulations [17]. We use this freedom to adjust the horizontal scale of the simulation data in Fig. 2 to give the best match between theory and simulation at intermediate to large $x$. The same scaling factor is used to rescale the simulation data in the other three figures. It is amusing to see that in Fig. 3 this rescaling causes the minima of the simulation data and the theoretical curve for the earlier theory [2] to coincide. No such rescaling of the experimental data was necessary. Figures 1 and 2 show reasonable agreement between the theoretical curve and the data from experiment and simulation

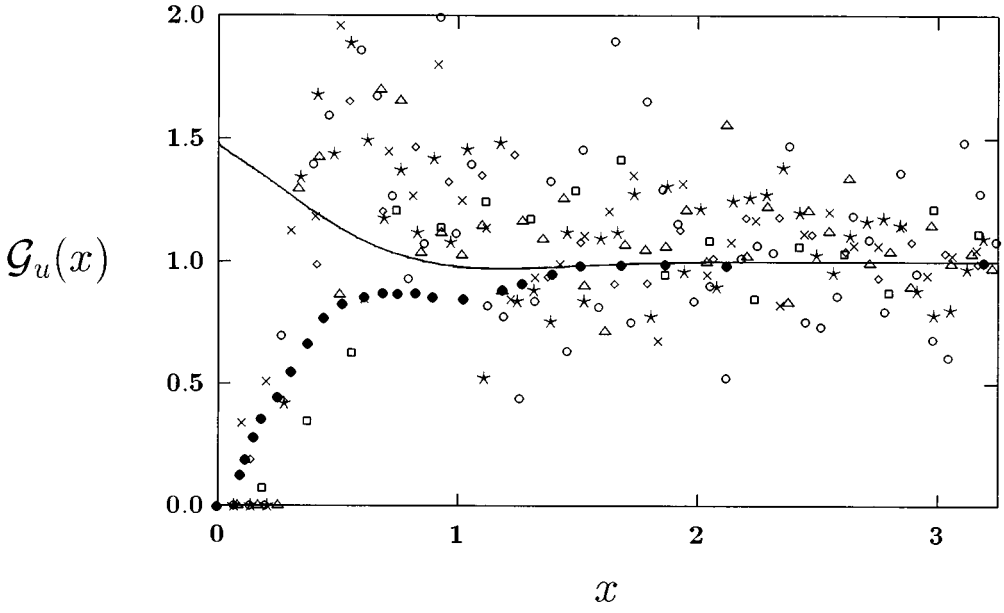


FIG. 4. The scaling form $\mathcal{G}_u$ (3.18) as a function of the scaled length $x=r/L(t)$ for the unsigned vortex correlation function of the two-dimensional O(2) model. The solid curve and the symbols are defined as in Fig. 1.

except for the short-distance behavior of $C_{va}$. This discrepancy is directly related to the behavior of $\mathcal{G}_s$. Since we know that the theoretical expression for $\mathcal{G}_s$ satisfies the sum rule (3.24), the question is whether this sum rule is satisfied by the simulation and experimental data. We have found that the simulation data presented in [5] lead to the result

$$-A\int d^dx\mathcal{G}_s(x)=0.85\pm 0.05, \tag{8.1}$$

which is less than the expected value of unity. We are able to compute this quantity directly from the data contained in Figs. 8 and 9 of [5], using the fact that in units of the scaling length they use in these figures $n_0(t)=L^{-2}$ so $A=1$. The error estimate in Eq. (8.1) is due to the uncertainties in reading the data, which is somewhat noisy, from the figures in [5]. Since the value for $A$ used in [6] is unknown and the data are noisy, we have not attempted to calculate whether the experimental data satisfy the sum rule. What could account for the breakdown in the sum rule seen in simulations? First, there is the possibility of a breakdown in scaling and a violation of the scaling relations (3.17) and (3.23). This seems incompatible with both experimental and simulation results when viewed as a function of time. A second, more likely, possibility is that there are some missing vortex-antivortex pairs in the simulations. We speculate that there may be a problem keeping track of annihilating pairs at short-scaled distances where they may have a very high relative velocity [18]. This problem, which might also occur in the experiments, may be the source of the short-distance discrepancy in $\mathcal{C}_{va}$ between the theory and the data from experiments and simulations.

## IX. CONCLUSION

Our work here has concentrated on the statistical properties of point vortices in phase ordering systems. The correlations among like-signed vortices found here meet with our expectation that vortices with the same charge repel one another at short-scaled distances and that screening of this repulsive interaction causes the correlations to fall rapidly to zero at large-scaled distances. The case of correlations between unlike-signed vortices seems straightforward from the theoretical point of view. Since these pairs are attractive there is an increasing probability of finding pairs on their way to annihilation as one goes to short-scaled distances. The experimental and simulation results seem at odds with this simple physical interpretation. One argument around the monotonic behavior of the vortex-antivortex correlation function is that the annihilating pair is speeding up in the late stage of annihilation and therefore the probability of finding the pair separated by a short distance is commensurately decreased. In recent calculations [19], using fundamentally the same theory as the one presented here, one of us found that a mechanism already exists in the theory to produce large vortex velocities. These large velocities are inferred from a power-law tail in the vortex velocity probability distribution. Bray [20] has shown that this tail results from scaling arguments applied to the late stages of the vortex-antivortex annihilation process. Thus it appears that this speeding up process is included in the present analysis.

In order to better understand the nature of the correlations between vortex-antivortex pairs, it would be instructive to work out the joint probability of having a vortex at position $\mathbf{r}$ with velocity $\mathbf{v}_2$ given that there is a vortex at the origin with velocity $\mathbf{v}_1$. This calculation is under current investigation.

One of the remaining unresolved questions is as follows: Where are the missing vortex-antivortex pairs in the experiments and simulations? Further progress is hindered until this discrepancy is understood.

## ACKNOWLEDGMENTS

The authors would like to thank T. Nagaya for supplying them with his experimental data. This work was supported in

part by the MRSEC Program of the National Science Foundation under Contract No. DMR-9400379. R.A.W. gratefully acknowledges support from the NSERC of Canada.

## APPENDIX A

We derive an expression for the reduced probability distribution,

$$G(\xi_1,\xi_2)=\left\langle \delta[\vec{m}(1)]\delta[\vec{m}(2)]\prod_{\mu\nu}\delta[(\xi_1)_\mu^\nu-\nabla_\mu m_\nu(1)] \times\delta[(\xi_2)_\mu^\nu-\nabla_\mu m_\nu(2)]\right\rangle \tag{A1}$$

appearing in the integral formula (6.2) for $\tilde{G}_u(\mathbf{r},t)$. We evaluate this Gaussian average for equal times $t_1=t_2=t$. The $\delta$ functions can be represented as integrals and one has

$$G(\xi_1,\xi_2)=\int\frac{d^nq_1}{(2\pi)^n}\frac{d^nq_2}{(2\pi)^n}\prod_{\mu\nu}\frac{d(k_1)_\mu^\nu}{2\pi}\frac{d(k_2)_\mu^\nu}{2\pi}\Gamma(\vec{q}_1,\vec{q}_2,k_1,k_2)\exp-i(k_j)_\mu^\nu(\xi_j)_\mu^\nu, \tag{A2}$$

where we have defined

$$\Gamma(\vec{q}_1,\vec{q}_2,k_1,k_2)=\langle\exp-i[\vec{q}_j\cdot\vec{m}(j)-(k_j)_\mu^\nu\nabla_\mu m_\nu(j)]\rangle. \tag{A3}$$

In these formulas summation over the repeated indices $\mu$, $\nu$, and $j$ is implied. The summation over $j$ is from 1 to 2, while the summation over $\mu$ and $\nu$ is from 1 to $n$, unless stated otherwise. Expression (A3) is of the standard form for Gaussian integrals

$$\left\langle\exp\left(\int d\overline{1}\vec{H}(\overline{1})\cdot\vec{m}(\overline{1})\right)\right\rangle=\exp\left(\frac{1}{2}\int d\overline{1}d\overline{2}\vec{H}(\overline{1})\cdot\vec{H}(\overline{2})C_0(\overline{12})\right), \tag{A4}$$

so a straightforward calculation yields

$$2\ln\Gamma(\vec{q}_1,\vec{q}_2,k_1,k_2)=-S_0\sum_j\vec{q}_j^{\,2}-S^{(2)}\sum_{\mu\nu j}[(k_j)_\mu^\nu]^2-2C_0\vec{q}_1\cdot\vec{q}_2+2\Big[C_0'[(k_1)_\mu^\nu q_2^\nu\hat{r}_\mu-(k_2)_\mu^\nu q_1^\nu\hat{r}_\mu] +\left(C_0''-\frac{C_0'}{r}\right)(k_1)_\mu^\alpha(k_2)_\nu^\alpha\hat{r}_\mu\hat{r}_\nu+\frac{C_0'}{r}(k_1)_\mu^\nu(k_2)_\mu^\nu\Big], \tag{A5}$$

where primes indicate differentiation with respect to $r$. This expression can be clarified if we introduce the orthogonal matrices $\hat{M}_\mu^\nu$ where

$$\hat{M}_\alpha^\mu\hat{M}_\alpha^\nu=\hat{M}_\mu^\alpha\hat{M}_\nu^\alpha=\delta_{\mu\nu} \tag{A6}$$

and

$$\hat{M}_1^\mu=\hat{r}_\mu, \tag{A7}$$

and then transform to the new variables $(W_j)_\mu^\nu$ defined by

$$(W_j)_\mu^\nu=\hat{M}_\alpha^\mu(k_j)_\alpha^\nu. \tag{A8}$$

We then obtain

$$\Gamma(\vec{q}_1,\vec{q}_2,W_1,W_2)=\exp\{-\tfrac{1}{2}[A(\vec{q}_1,\vec{q}_2)+A_L((\vec{W}_1)_L,(\vec{W}_2)_L)+A_T((W_1)_T,(W_2)_T)+A_c(\vec{q}_1,\vec{q}_2,(\vec{W}_1)_L,(\vec{W}_2)_L)]\}, \tag{A9}$$

where $(W_j)_L^\nu=(W_j)_1^\nu$ is the longitudinal part of $W_j$ and $(W_j)_T$ is shorthand notation referring to the remaining transverse parts of $W_j$ [$(W_j)_\mu^\nu$ with $\mu>1$]. With this choice of variables we notice that $\Gamma$ can be factored into a transverse and a longitudinal piece. We see that for our purposes we are not required to be more explicit than Eqs. (A6) and (A7) in defining the $\hat{M}_\mu^\nu$. The quantities appearing in the exponential in Eq. (A9) are

$$A(\vec{q}_1,\vec{q}_2)=S_0\sum_j\vec{q}_j^{\,2}+2C_0\vec{q}_1\cdot\vec{q}_2, \tag{A10}$$

$$A_L((\vec{W}_1)_L,(\vec{W}_2)_L)=S^{(2)}\sum_j[(\vec{W}_j)_L]^2-2C_0''(\vec{W}_1)_L\cdot(\vec{W}_2)_L, \tag{A11}$$

$$A_T((W_1)_T,(W_2)_T)=-2\frac{C_0'}{r}\sum_{\mu=2}\sum_{\nu}(W_1)_\mu^\nu(W_2)_\mu^\nu+S^{(2)}\sum_{\mu=2}\sum_{\nu j}[(W_j)_\mu^\nu]^2, \tag{A12}$$

$$A_c(\vec{q}_1,\vec{q}_2,(\vec{W}_1)_L,(\vec{W}_2)_L)=2C_0'[\vec{q}_1\cdot(\vec{W}_2)_L-\vec{q}_2\cdot(\vec{W}_1)_L]. \tag{A13}$$

One can integrate Eq. (A9) over $\vec{q}_1$ and $\vec{q}_2$ to obtain

$$\Gamma(W_1,W_2)=\int\frac{d^nq_1}{(2\pi)^n}\frac{d^nq_2}{(2\pi)^n}\Gamma(\vec{q}_1,\vec{q}_2,W_1,W_2)=\left(\frac{\gamma}{2\pi S_0}\right)^n\exp\left(-\frac{1}{2}[A_L'((\vec{W}_1)_L,(\vec{W}_2)_L)+A_T((W_1)_T,(W_2)_T)]\right), \tag{A14}$$

where we define

$$A_L'((\vec{W}_1)_L,(\vec{W}_2)_L)=S_L\sum_j[(\vec{W}_j)_L]^2+2C_L(\vec{W}_1)_L\cdot(\vec{W}_2)_L, \tag{A15}$$

with $S_L$ and $C_L$ given by Eqs. (6.9) and (6.10), respectively. Since the transformation (A8) is orthogonal we have the simple result for $G$,

$$G(t_1,t_2)=\left(\frac{\gamma}{2\pi S_0}\right)^n G_L((\vec{t}_1)_L,(\vec{t}_2)_L)G_T((t_1)_T,(t_2)_T) \tag{A16}$$

depending on the rotated variable

$$(t_j)_\mu^\nu=\hat{M}_\beta^\mu(\xi_j)_\beta^\nu. \tag{A17}$$

The longitudinal and transverse parts of $t$ are defined in analogy to those of $W$. The functions $G_L$ and $G_T$ appearing in Eq. (A16) are explicitly given in Eqs. (6.7) and (6.8).

## APPENDIX B

In this appendix we compute the integral

$$J(\vec{s}_1,\vec{s}_2)=\int d^2xd^2y|s_{11}x_2-s_{12}x_1||s_{21}y_2-s_{22}y_1|\exp\left(-\frac{1}{2}[\vec{x}^2+\vec{y}^2-2f_T\vec{x}\cdot\vec{y}]\right), \tag{B1}$$

which is needed to evaluate $\mathcal{G}_u(\mathbf{r},t)$ for $n=d=2$. The $j$th component of $\vec{s}_i$ is written $s_{ij}$. To rid ourselves of the absolute values appearing in Eq. (B1) we make use of the identity

$$|x|=\int_{-\infty}^{+\infty}\frac{dz}{\sqrt{2\pi}}\left(-\frac{1}{z}\frac{\partial}{\partial z}\right)e^{-x^2z^2/2} \tag{B2}$$

and write

$$J(\vec{s}_1,\vec{s}_2)=\int_{-\infty}^{+\infty}\frac{dz_1}{\sqrt{2\pi}}\frac{dz_2}{\sqrt{2\pi}}\frac{1}{z_1z_2}\frac{\partial^2}{\partial z_1\partial z_2}\int d^2xd^2y\exp\left(-\frac{1}{2}A(z_1,z_2,\vec{s}_1,\vec{s}_2,\vec{x},\vec{y})\right), \tag{B3}$$

with

$$A(z_1,z_2,\vec{s}_1,\vec{s}_2,\vec{x},\vec{y})=z_1^2(s_{11}x_2-s_{12}x_1)^2+z_2^2(s_{21}y_2-s_{22}y_1)^2+\vec{x}^2+\vec{y}^2-2f_T\vec{x}\cdot\vec{y}. \tag{B4}$$

The integrations over $\vec{x}$ and $\vec{y}$ in Eq. (B3) are Gaussian and so can be readily, if somewhat tediously, performed. One has

$$J(\vec{s}_1,\vec{s}_2)=\int_{-\infty}^{+\infty}\frac{dz_1}{\sqrt{2\pi}}\frac{dz_2}{\sqrt{2\pi}}\frac{1}{z_1z_2}\frac{\partial^2}{\partial z_1\partial z_2}\frac{(2\pi)^2}{\sqrt{D(z_1,z_2,\vec{s}_1,\vec{s}_2)}}, \tag{B5}$$

where the determinant $D$ is given by

$$D=(1+z_2^2\vec{s}_2^{\,2})(1+z_1^2\vec{s}_1^{\,2})-f_T^2(2+z_1^2\vec{s}_1^{\,2}+z_2^2\vec{s}_2^{\,2}+z_1^2z_2^2[\vec{s}_1\cdot\vec{s}_2]^2)+f_T^4. \tag{B6}$$

The next step is to evaluate the derivatives with respect to $z_1$ and $z_2$ appearing in Eq. (B5). This can be done straightforwardly, and one notices that a change of variables allows one to write the integral in Eq. (B5) as a product of the amplitudes of $\vec{s}_1$ and $\vec{s}_2$ and an integral whose only dependence on $\vec{s}_1$ and $\vec{s}_2$ is through the dot-product form

$$g = f_T^2 (\hat{s}_1 \cdot \hat{s}_2)^2. \tag{B7}$$

Explicitly, one has

$$J(\vec{s}_1, \vec{s}_2) = 2\pi \gamma_T^4 |\vec{s}_1||\vec{s}_2| \widetilde{J}(g) \tag{B8}$$

with

$$\widetilde{J}(g) = \int_{-\infty}^{+\infty} dy_1 dy_2 \frac{[1+2g+(1-g)(y_1^2+y_2^2)+(1-g)^2 y_1^2 y_2^2]}{[1+y_1^2+y_2^2+(1-g)y_1^2 y_2^2]^{5/2}}. \tag{B9}$$

This seemingly complex integral for $\widetilde{J}(g)$ is actually pleasingly simple and after some manipulations one has

$$\widetilde{J}(g) = 4\sqrt{1-g} + 4\sqrt{g} \tan^{-1} \sqrt{\frac{g}{1-g}}. \tag{B10}$$

## APPENDIX C

To examine the small-$x$ behavior of the defect correlation functions we need to know the behavior of $f$, $f_T$, and $f_L$ for small $x$. In the theory we use here, which is discussed in detail in [4], $f$ is analytic at short-scaled distances and we have

$$f(x) = 1 - \alpha x^2 + \beta x^4 + \cdots, \tag{C1}$$

where $\alpha$ and $\beta$ are constants determined in the theory. To evaluate $f_T$ we write $C_T$ (6.14) in terms of $f$, as a function of the scaled length $x$:

$$C_T = -\frac{S_0}{L^2} \frac{f'}{x} = -\frac{1}{2d\alpha} \frac{f'}{x}, \tag{C2}$$

where we have used the result $S_0/L^2 = 1/2d\alpha$ [4]. The result (C2), together with the definition (6.13) for $S_T$ and the expansion (C1) lead to

$$f_T \equiv \frac{C_T}{S_T} = 1 - \frac{2\beta}{\alpha} x^2 + \cdots \tag{C3}$$

for small $x$. We now examine $f_L$ in the scaling regime and use Eqs. (6.9) and (6.10) to write

$$S_L = \frac{1}{d} - \frac{1}{2d\alpha} \gamma^2 (f')^2 \tag{C4}$$

and

$$C_L = -\frac{1}{2d\alpha} [f'' + f\gamma^2 (f')^2]. \tag{C5}$$

For small $x$ we again use (C1) and obtain

$$f_L \equiv \frac{C_L}{S_L} = -1 + O(x^2). \tag{C6}$$

The key results here are $f_T \to 1$ while $f_L \to -1$ when $x \to 0$. This minus sign is ultimately responsible for the relation

$$\mathcal{G}_s(0) = -\mathcal{G}_u(0) \tag{C7}$$

between the signed and unsigned defect correlation functions at $x = 0$ [21].


[1] For a review of topological defects in ordered media, see N. D. Mermin, Rev. Mod. Phys. **51**, 591 (1979).

[2] F. Liu and G. F. Mazenko, Phys. Rev. B **46**, 5963 (1992).

[3] F. Liu and G. F. Mazenko, Phys. Rev. B **45**, 6989 (1992).

[4] G. F. Mazenko and R. A. Wickham, Phys. Rev. E **55**, 1321 (1997).

[5] M. Mondello and N. Goldenfeld, Phys. Rev. A **42**, 5865 (1990).

[6] T. Nagaya, H. Orihara, and Y. Ishibashi, J. Phys. Soc. Jpn. **64**, 78 (1995).

[7] Scaling in the O($n$) model is believed to be controlled by a zero-temperature fixed point. Near the fixed point, temperature is an irrelevant variable and is not expected to affect the scaling exponents or the leading order form for the scaling functions. Z. W. Lai, G. F. Mazenko, and O. T. Valls, Phys. Rev. B **37**, 9481 (1988); A. J. Bray, Phys. Rev. Lett. **62**, 2841 (1989); Phys. Rev. B **41**, 6724 (1990).

[8] For a recent review see A. J. Bray, Adv. Phys. **43**, 357 (1994).

[9] There is theoretical and numerical evidence, however, for logarithmic corrections to the growth law when $n = d = 2$. It appears that $L \sim (t/\ln t)^{1/2}$. B. Yurke, A. N. Pargellis, T. Kovacs, and D. A. Huse, Phys. Rev. E **47**, 1525 (1993); A. D. Rutenberg and A. J. Bray, *ibid.* **51**, 5499 (1995). We see only the $L \sim t^{1/2}$ growth law for $n = d = 2$ in the theory presented here.

[10] B. I. Halperin, in *Physics of Defects*, edited by R. Balian *et al.* (North-Holland, Amsterdam, 1981).

[11] We assume overall topological charge neutrality so $\langle \rho(1) \rangle = \Sigma_\alpha q_\alpha = 0$.

[12] G. F. Mazenko, Phys. Rev. B **42**, 4487 (1990).
[13] G. Porod, in *Small Angle X-Ray Scattering*, edited by O. Glatter and L. Kratky (Academic, New York, 1982).
[14] The Gaussian approximation is the basis for most analytical theories of phase ordering. For a discussion of how the Gaussian approximation fits into a more general and systematic scheme of approximations, see G. F. Mazenko, Phys. Rev. E **49**, 3717 (1994); G. F. Mazenko, *ibid.* **50**, 3485 (1994); R. A. Wickham and G. F. Mazenko, *ibid.* **55** 2300 (1997).
[15] A. J. Bray and S. Puri, Phys. Rev. Lett. **67**, 2670 (1991); H. Toyoki, Phys. Rev. B **45**, 1965 (1992).
[16] The factor of $(8\mu/S^{(2)})^n\Gamma^2(1+n/2)/(n!)^2$, not present in earlier formulas for $\mathcal{G}_s$ [2,4], appears in Eq. (5.2) because in this paper the time-dependent amplitude relating the unscaled quantity $\tilde{G}_s$ to the scaled quantity $\mathcal{G}_s$ is $[n_0(t)]^2$ instead of $L^{-2n}$.
[17] Previously, when comparing theory and simulation for the signed vortex correlation function [2,4] appearing in Fig. 3, the amplitude of the simulation curve was a second free fitting parameter. Here, the relation between the theoretical, experimental, and simulation amplitudes is fixed because the defect density is used to normalize the curves.
[18] An additional consideration is that the vortex cores in the simulation are found to be eight lattice sites wide, a distance comparable to the position of the peak in Fig. 9 of [5].
[19] G. F. Mazenko, Phys. Rev. Lett. **78**, 401 (1997).
[20] A. J. Bray, Phys. Rev. E **55**, 5297 (1997).
[21] One caveat is that the results of Appendix C follow from the small-$x$ expansion (C1) for $f$. In [4] the proper treatment of fluctuations allowed us to use this expansion for $n=d=2$. We expect to be able to extend [4] and construct $f$ to be analytic to $O(x^4)$ for $n>2$.